Supplemental Figure legend

FIGURE S1. Expression pattern of *atg-4.1::gfp*

(A-D) The *atg-4.1::gfp* reporter functionally rescues defective degradation of SEPA-1 aggregates in *atg-4.1* mutants. SEPA-1 aggregates accumulate in late stage *atg-4.1* mutant embryos, but are almost completely absent in late stage *atg-4.1* mutant embryos carrying the *atg-4.1::gfp* transgene. (A) and (C): Nomarski images of the embryos shown in (B) and (D), respectively.

(E and F) *atg-4.1::gfp* is ubiquitously expressed in the cytoplasm in embryos. (E) Nomarski image of the embryo in (F).

(G and H) Expression of *atg-4.1::gfp* remains unchanged in *atg-4.2(tm3948)* mutant embryos. (G) Nomarski image of the embryo in (H).

(I and J) Real-time PCR results show that mRNA levels of *atg-4.2* and *atg-4.1* are not changed in *atg-4.1* (I) and *atg-4.2* mutants (J), respectively.

FIGURE S2. Alignment of ATG-4.1 and ATG-4.2 with yeast Atg4p and human Atg4B

Clustal X (version 1.83) alignment of *Ce*ATG-4.1(NP_493375), *Ce*ATG-4.2(NP_502208), *Sc*Atg4p(NP_014176), and *Hs*Atg4B(NP_037457). The catalytic site, the regulatory loop and the mutated residues found in *atg-4.1* mutants are marked.

FIGURE S3. ATG-4.2 does not reduce the catalytic efficiency of ATG-4.1

(A-B) Different ratios (1:0, 1:1, and 1:5) of ATG-4.1 and ATG-4.2 in a fixed amount of total enzymes (0.0125 mg/ml) were incubated with decreasing concentrations of the substrate LGG-1-His_6 for 5 minutes. SDS-PAGE followed by CBB staining was used to resolve the mixture. The curves were plotted and fitted as described in Fig. 4G-J.

(C) The efficiency (k_{cat}/Km) of each reaction catalyzed by different ratios of enzyme mixture (ATG-4.1 to ATG-4.2) was calculated as described in Fig. 4K. The value of the reaction without ATG-4.2 was considered as the basal efficiency of ATG-4.1. The enzyme mixture exhibited a slightly increased efficiency in cleaving the substrates as expected from the same concentration of ATG-4.1 alone.

FIGURE S4. Accumulation of SEPA-1 aggregates and LGG-1 puncta in *epg-6*, *atg-4.1*, and their double mutants

This figure shows separate images for Fig. 6F,G,H.

(A-D) SEPA-1 aggregates and LGG-1 puncta form clusters and are largely colocalized in *epg-6* mutant.

(E-H) In *atg-4.1* mutants, SEPA-1 aggregates are small and separable from LGG-1 puncta.

(I-L) In *atg-4.1; epg-6* double mutants, SEPA-1 aggregates are small, spherical and do not colocalize with LGG-1 puncta, resembling those in *atg-4.1* mutants.

(A), (E) and (I): DAPI image of the embryo shown in the same row.

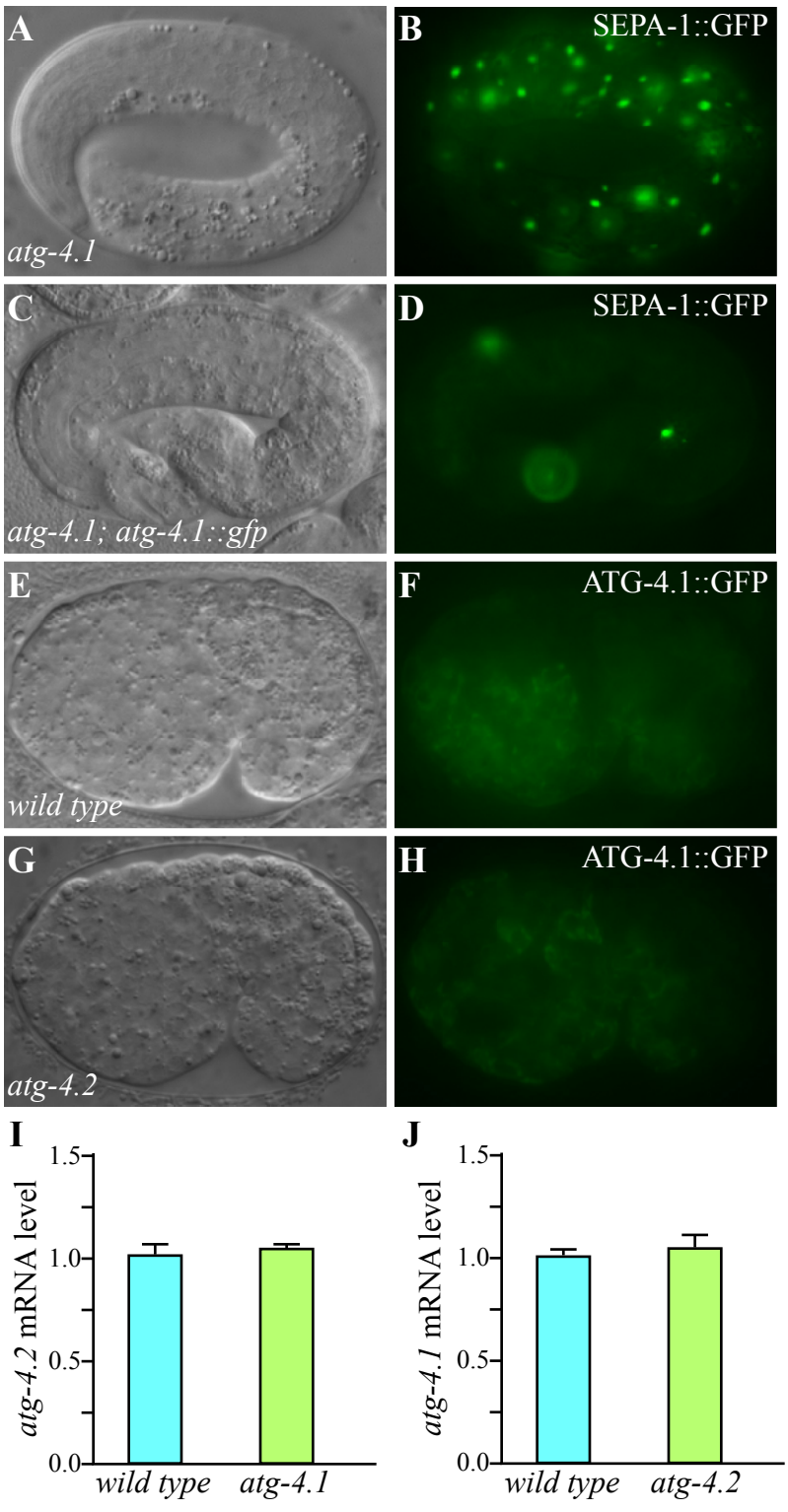
A
atg-4.1
B
SEPA-1::GFP
C
atg-4.1; atg-4.1::gfp
D
SEPA-1::GFP
E
wild type
F
ATG-4.1::GFP
G
atg-4.2
H
ATG-4.1::GFP
I
atg-4.2 mRNA level
1.5
1.0
0.5
0.0
wild type
atg-4.1
J
atg-4.1 mRNA level
1.5
1.0
0.5
0.0
wild type
atg-4.2

Figure S1

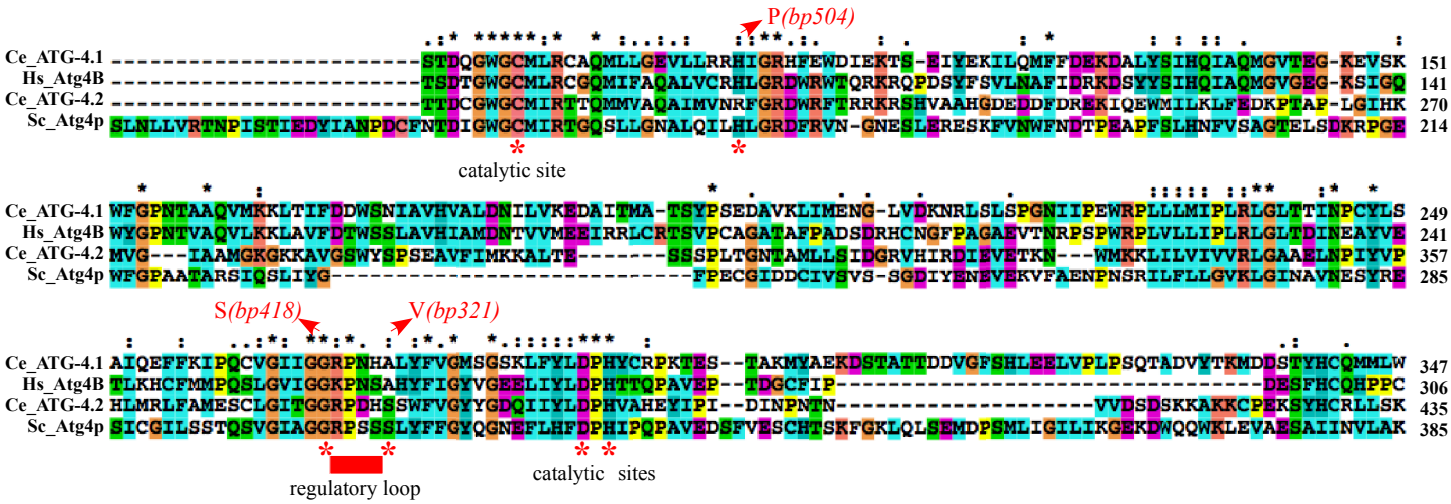
P(bp504)
Ce_ATG-4.1
Hs_Atg4B
Ce_ATG-4.2
Sc_Atg4p
catalytic site
S(bp418)
V(bp321)
regulatory loop
catalytic sites

Figure S2

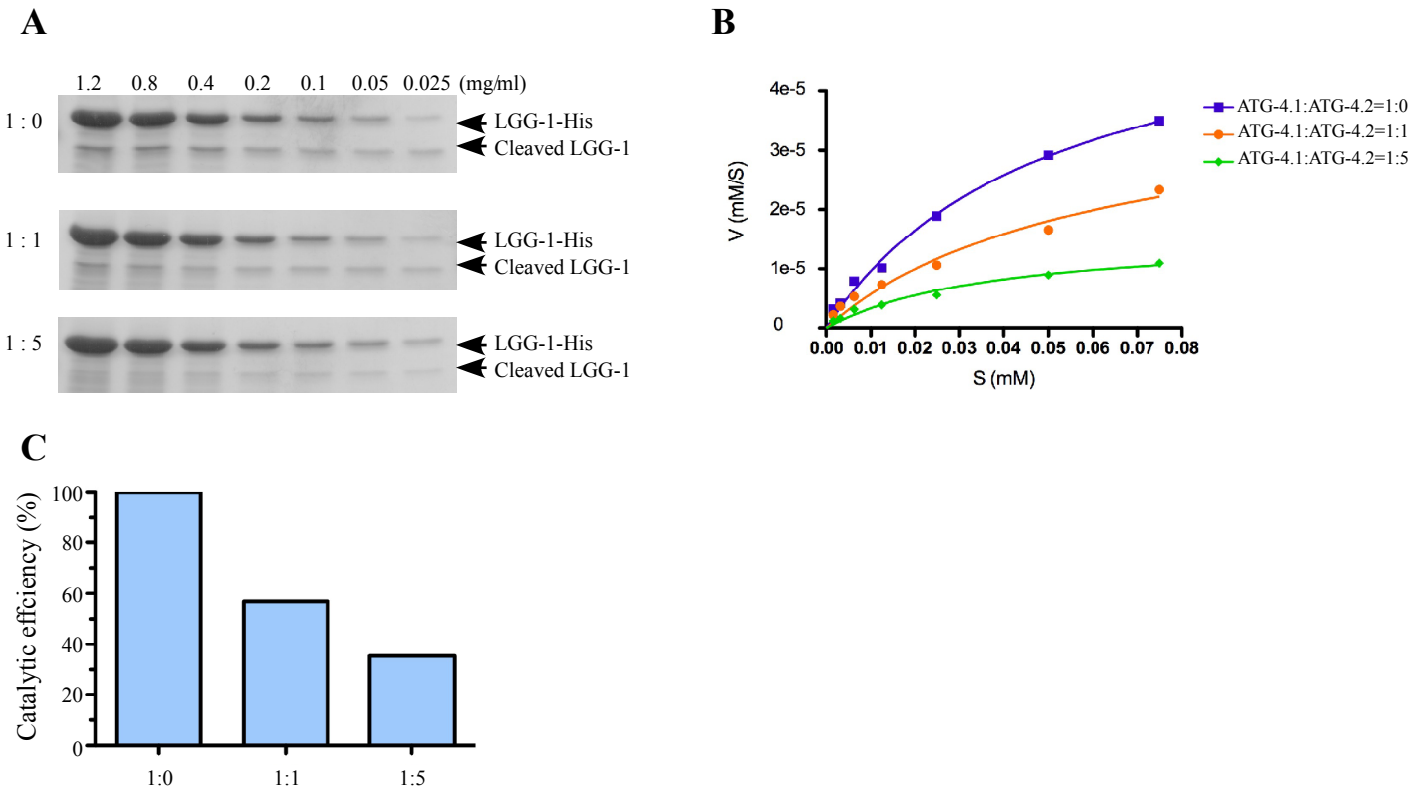
A
1.2 0.8 0.4 0.2 0.1 0.05 0.025 (mg/ml)
1 : 0
LGG-1-His
Cleaved LGG-1
1 : 1
LGG-1-His
Cleaved LGG-1
1 : 5
LGG-1-His
Cleaved LGG-1
B
4e-5
3e-5
2e-5
1e-5
0
V (mM/S)
0.00 0.01 0.02 0.03 0.04 0.05 0.06 0.07 0.08
S (mM)
ATG-4.1:ATG-4.2=1:0
ATG-4.1:ATG-4.2=1:1
ATG-4.1:ATG-4.2=1:5
C
Catalytic efficiency (%)
100
80
60
40
20
0
1:0
1:1
1:5

Figure S3

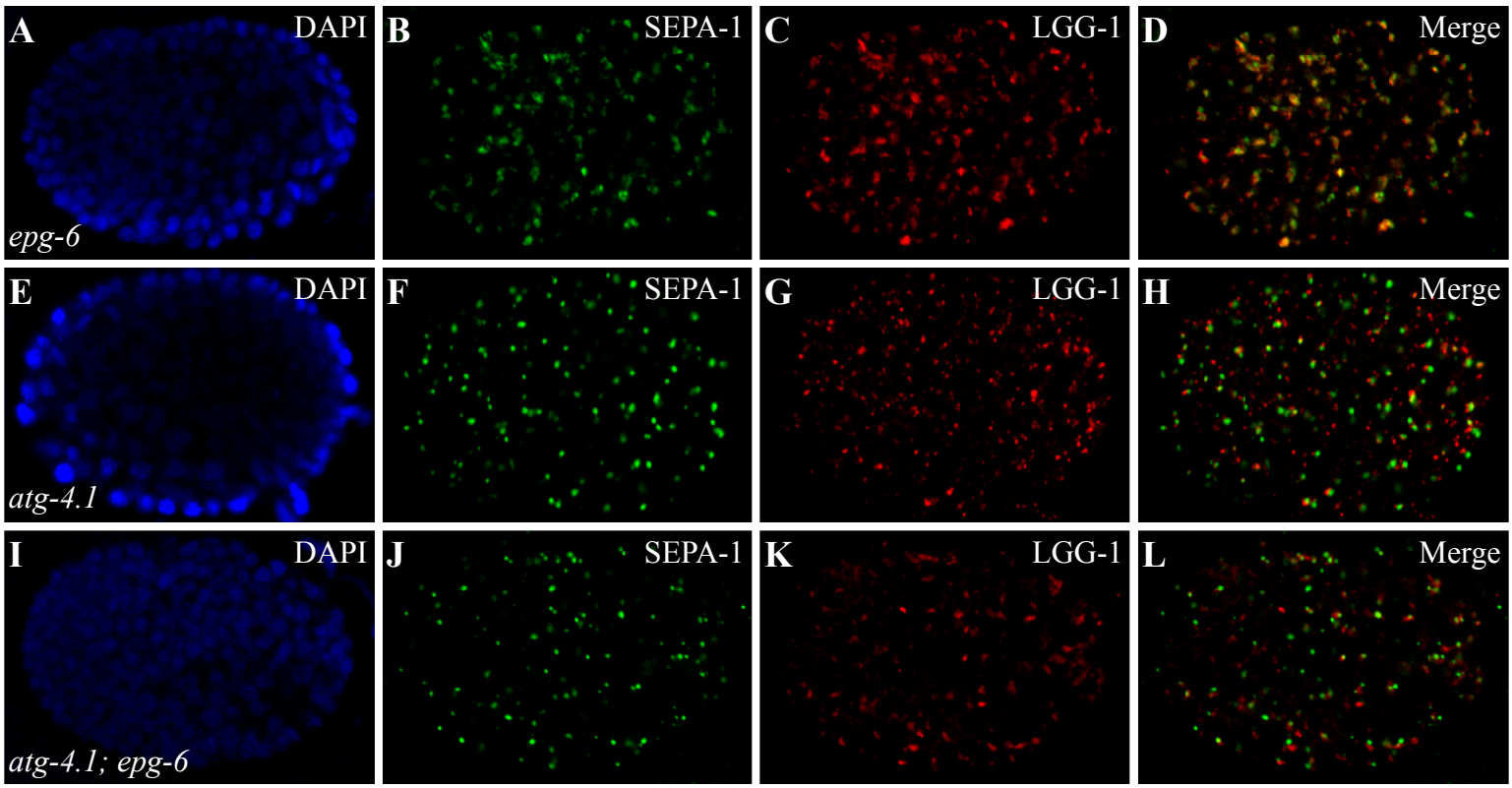
A
DAPI
epg-6
B
SEPA-1
C
LGG-1
D
Merge
E
DAPI
atg-4.1
F
SEPA-1
G
LGG-1
H
Merge
I
DAPI
atg-4.1; epg-6
J
SEPA-1
K
LGG-1
L
Merge

Figure S4